Energy Technology
Generation, Conversion, Storage, Distribution
www.entechnol.de

CO_2 Methanation on Hydrotalcite-Derived Catalysts and Structured Reactors: A Review

*Huong Lan Huynh and Zhixin Yu**

CO_2 methanation reaction has attracted renewed interest since the power-to-gas (PtG) concept emerged as a promising alternative for CO_2 emission abatement using surplus renewable electricity. Although the reaction has been reported for more than a century, improvements in the catalytic system and reactor design remain challenging. Recently, hydrotalcite (HT) materials known for their facile synthesis and high performance are extensively used as precursors for supported catalysts in a wide range of reactions, including CO_2 hydrogenation to CH_4. Herein, a comprehensive overview on HT-derived catalysts applied for CO_2 methanation is provided. More importantly, new reactor concepts are extensively investigated, such as honeycomb and microchannel reactors, to overcome issues related to the high exothermic nature of the reaction. The latest achievements with respect to structured reactors are also comprehensively reviewed and thoroughly discussed.

1. Introduction

Society is struggling to meet the ambitious goals of reducing carbon emissions. In fact, in 2018, the global carbon emissions grew by 2.0%, the fastest growth since 2010.[1] Currently, electricity production and heat generation emit the largest amount of CO_2, accounting for 42% of global CO_2 emissions.[2] Regardless of the climate change controversy, our energy system is inevitably in transition from fossil fuel to renewable energy sources (RES) as one of the primary power sources. In Europe, a shift toward RES is observed by an increasing share of wind, solar, and biomass sources in the gross electricity production, from 20% in 2010 to 32% in 2018.[3,4] It is expected that half of the electricity in the European power sector will be generated by RES in 2030. However, RES is intermittent and unpredictable, resulting in a seasonal surplus of electricity that requires a flexible storage system. Power-to-gas (PtG) concept, a potential chemical energy storage system, is one of the promising solutions. The concept is to convert the excessive electrical power into a gaseous energy carrier, such as hydrogen (H_2) and/or methane (CH_4), via a two-step process: H_2 production by water electrolysis and H_2 conversion to CH_4 by methanation reaction with external CO_2 sources.[4,5] The existing well-established natural gas network in Europe is one of the advantages to distribute and store synthetic CH_4. Moreover, the large scale of CO_2 emissions can be recycled in this PtG process.

$$CO_2 + 4H_2 \leftrightarrow CH_4 + 2H_2O \quad \Delta H = -165.0\,\text{kJ mol}^{-1} \tag{1}$$

CO_2 methanation, also called the Sabatier reaction (Equation (1)), was discovered in 1902.[6] Industrially, methanation was applied to remove traces of CO and CO_2 gases from the H_2-rich stream for ammonia plants, for instance. During the oil crisis in the 1970s, the reaction was further investigated for the production of synthetic natural gas (SNG).[5] However, only a few projects reached a commercial scale because of technical difficulties. Problems relating to reactor concept selection, cleaning reactant gases to avoid catalyst deactivation, process efficiency, and economical attractiveness, etc. have been challenging for the SNG projects. Recently, CO_2 methanation underwent a revival as it is an essential part of the PtG process that offers an alternative for renewable electricity storage and facilitates' industrial decarbonization. In addition, the reaction is also appealing for long-term space exploration missions by space agencies, such as the National Aeronautics and Space Administration (NASA), which has used the Sabatier reaction for Mars exploration.[7]

Depending on the catalyst used, typical operating conditions are temperatures of 200–550 °C and pressures of 1–100 bar.[8] In terms of thermodynamics, the exothermic Sabatier reaction is favored at high pressures and low temperatures.[9] Due to kinetic limitations, maximum CO_2 conversion and CH_4 production are only achieved at high temperatures and pressures. A comprehensive review on the kinetics of CO_2 methanation with kinetic models over Ni-, Ru-, and Cu-based catalysts has been reported.[10] However, operation at high pressures is not practically economical, whereas operation at low temperatures requires highly active catalysts. Hence, the primary research on CO_2 methanation focuses on the exploration of new active materials and reactor design with regard to the improvement of heat and mass transfer. Furthermore, the Sabatier reaction itself is a well-developed process, yet there are controversial arguments on the reaction mechanism, mainly due to uncertainties on the intermediates

H. L. Huynh, Prof. Z. Yu
Department of Energy and Petroleum Engineering
University of Stavanger
4036 Stavanger, Norway
E-mail: zhixin.yu@uis.no

The ORCID identification number(s) for the author(s) of this article can be found under https://doi.org/10.1002/ente.201901475.

DOI: 10.1002/ente.201901475

formed during the reaction.[10–13] CH_4 from CO_2 hydrogenation could be formed by the dissociation of CO_2 to CO, either via a direct C—O bond cleavage (carbide pathway) or via formate intermediate. In addition, CH_4 formation through carboxyl intermediate has also been reported.

Many metals in group VIII in the periodic table, e.g., Ni, Co, Fe, Ru, Rh, etc., are active for the methanation reaction.[11,14] Although noble metals like Ru showed excellent activity and selectivity, the Earth-abundant Ni-based catalysts have always been the first choice for industrial applications due to its availability and affordable price. However, Ni-based catalysts exhibited a poor catalytic activity below 350 °C.[13] Catalytic activity at low temperatures is dependent not only on the Ni active metal but also on various factors, e.g., supports, promoters, preparation conditions, reduction, activation, etc. Studies revealed that high dispersion of metallic active sites on suitable support greatly contributes to the activation and dissociation of H_2 molecules. Thus, oxide supports with a high surface area, like SiO_2, Al_2O_3, SiO_2–Al_2O_3, and zeolites, are commonly used to obtain highly dispersed Ni-based catalysts. Many other oxides have also been studied (e.g., CeO_2, α-Al_2O_3, TiO_2, MgO, CeO_2/ZrO_2, etc.) as promising supports.[15] As different materials with unique physiochemical properties can positively influence the catalytic properties, the combination of two or more compounds could be beneficial for catalysis development.

Moreover, surface basicity can be tuned to enhance the chemisorption and dissociation of CO_2 molecules. Alkaline Earth oxides, such as MgO, are usually used to strengthen the basicity of the catalytic surface. The combination of MgO and Al_2O_3, as anticipated, has been reported as the best support for CO_2 conversion reactions, such as dry reforming, due to its high basicity, large surface area, and pore volume.[16] Metal sintering and carbon deposition are other challenges of Ni-based catalysts in CO_2 methanation. Due to the exothermic feature of the reaction, hotspots possibly occur in the catalytic bed and can cause thermal agglomeration of metallic Ni active sites. Consequently, it reduces the stability of the catalysts. To address these problems, Ni active sites are often stabilized by well-defined crystalline structures (i.e., solid solution, spinel, perovskite, etc.), rigid mesoporous frameworks, or core–shell structures.[17]

A critical component of CO_2 methanation technology is to synthesize highly active and stable catalysts, based on the strategies discussed earlier. Much efforts from both academia and industry are focused on the development of the methanation catalysts and process technology. This is witnessed by the number of review papers dedicated to this process, which have covered general aspects of methanation,[9,13,17,18] reaction mechanism,[10,12,19] supported catalysts,[14,15] plasma-catalytic process,[20] etc. Among these, hydrotalcite (HT)-derived catalysts have emerged as promising catalytic material for CO_2 conversion reactions, particularly CO_2 methanation and CO_2 reforming of methane. A special review paper on HT-derived catalysts for CO_2 reforming of methane has been published.[21] To complement the aforementioned review, we first review the applications of HT-derived Ni-based catalysts for CO_2 methanation in this work, due to the specific features and performance of these catalyst materials. Furthermore, reactor design is another important focus for the commercialization of the Sabatier process. Heat management plays a key role to achieve high CO_2 conversion in this highly exothermic reaction.

Huong Lan Huynh received her B.Sc. degree in chemical engineering from Vietnam National University—Ho Chi Minh City University of Technology (Vietnam) in 2016. She obtained her M.Sc. degree in natural gas technology from the University of Stavanger (Norway) in 2018. Currently, she is a Ph.D. candidate at the same university. Her research interest is heterogeneous catalysis and chemical processes for CO_2 conversion.

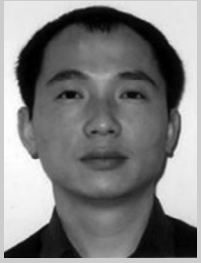

Zhixin Yu obtained his B.Sc. degree in applied chemistry from University of Science and Technology of China (USTC) in 1998, M.Sc. degree in manufacturing management from Linköping University (Sweden) in 2001, and Ph.D. degree in chemical engineering from Norwegian University of Science and Technology (Norway) in 2005. He joined the University of Stavanger (Norway) as professor in Natural Gas Technology in 2013. His main research interests include nanomaterials and nanotechnology for petroleum and clean energy production, nanocatalysis, syngas and H_2 production, biogas production, CO_2 conversion and utilization, etc.

Structured catalysts and reactors are among the best solutions to address this challenge. In the second part of this Review, we will discuss in more detail the latest progress on structured catalysts and reactors, which has not been covered by other reviews.

2. HTs as Precursors for Supported Catalysts

HT-like materials are also called layered double hydroxides (LDHs), which have similar structures as natural magnesium–aluminum hydroxycarbonate. The general formula for LDH material is $[M_{1-x}^{2+}M_x^{3+}(OH)_2](A^{n-})_{x/n}\cdot mH_2O$, where M represents metals and A is the anion. The value of x (molar ratio of trivalent and divalent cations) is preferred to be in the range of 0.2–0.4 to obtain a pure LDH phase and avoid the formation of hydroxides and other compounds. Divalent cations can be Mg and/or other metals (e.g., Fe, Co, Cu, Ni, or Zn), whereas trivalent cations are Al and/or other metals (e.g., Cr, Ga, In, Mn, or Fe).[22] Because a wide range of cations and anions can be incorporated, HT-like precursors have drawn much attention as promising materials for heterogeneous catalyst design. As the cations in HT structures are well dispersed, the obtained mixed oxides upon thermal decomposition usually show a good distribution of metal active sites. Therefore, derivatives of HT-like precursors after calcination are often used as supported metal catalysts.[23] The phase transformations during calcination of the HT precursors and subsequent reduction of the mixed oxides are schematically shown in **Figure 1**. Another important feature of HT-derived catalysts is the tunable basic strength

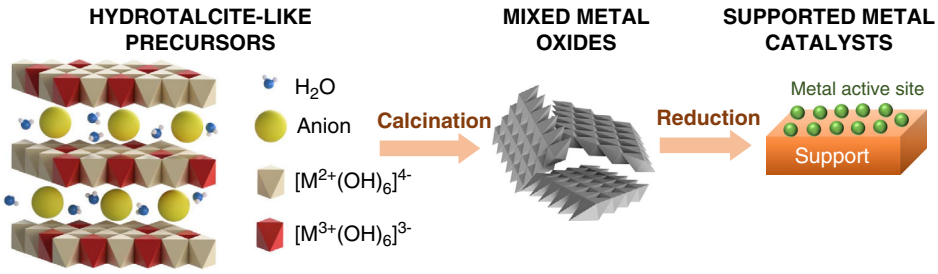

Figure 1. Preparation pathway of supported metal catalysts from HT-like precursors.

through judicious choices of metal cations and compositions, to achieve desirable activity and selectivity for specific catalytic reactions. Therefore, HT-derived catalysts have been extensively applied in many reactions, including hydrogenation and hydrodesulfurization, polymerizations, syngas production from steam reforming, dry reforming of methane, as well as the Sabatier reaction.[21,24]

2.1. Ni/Al_2O_3 Catalysts Derived from HT Materials

The main challenge in catalyst development for CO_2 methanation is to enhance the catalytic activity and stability for the Earth-abundant transition metal Ni. A higher CH_4 conversion can be achieved using high loading catalysts.[25] However, the catalyst may consequently possess low metal dispersion and is susceptible to sintering.[26] HT-derived catalysts can be an alternative solution because the calcined precursors have strong metal–support interaction and high dispersion of active metals, regardless of the metal loading. Regarding the application of HT-like materials for CO_2 methanation, Ni/Al_2O_3 HT-derived catalysts were first reported by Abelló et al.[27] Since then, there has been an increasing number of publications using Ni-based HT-derived catalysts for the Sabatier reaction, as shown in **Table 1**. In addition, different types of promoted catalysts were also included. The promoters could be a second metallic site (e.g., Fe and Co) or could be incorporated into the support structure (e.g., MgO, CeO_2, and La_2O_3). It was expected to enhance the basicity and/or improve Ni distribution for a better catalytic performance.

HT precursors are prepared by the conventional coprecipitation at constant pH, which is usually preferred at high pH (>8).[28] Aging or hydrothermal treatment is an additional step

Table 1. Summary of Ni-based HT-derived catalysts for CO_2 methanation.

HT-derived Catalysts	Ni loading [wt%]	$[M^2]^+/M^{3+}$	Reaction conditions			X_{CO2}[b)][%]	S_{CH4}[c)] [%]	Ref.
			T [°C]; P [bar][a)]	H_2:CO_2:standard gases ratio	Space velocity			
Ni/Al_2O_3	69.1	5	400; 10	4:1:1	268.8 L g_{cat}^{-1} h^{-1}	92.4	>99	[27]
Ni/Al_2O_3	75–76	3	300	10:2.5:87.5	20 000 h^{-1}	80–85	>97	[28]
Ni/Al_2O_3	78	3	350	72:18:10	75 L g_{cat}^{-1} h^{-1}	82.5	99.4	[29]
Ni/Al_2O_3	21.3–42.6	0.5–3	220	34.35:0.65:65	20 000 h^{-1}	–	–	[30]
Ni/Al_2O_3	–	2	275	4:1:1	≈107.5 L g_{cat}^{-1} h^{-1}	66	98.7	[31]
Ni/Al_2O_3	≈73	5	250	12:3:5	2400 h^{-1}	90	>99	[32]
Ni/Al_2O_3	75	3	350	40:10:50	30 000 h^{-1}	–	40	[33]
$Ni/MgAlO_x$	59	2	250	18.5:4.6:77	66 L g_{cat}^{-1} h^{-1}	20	18	[34]
$Ni/MgAlO_x$	10.3–42.5	3	250	12:3:5	12 000 h^{-1}	72	>99	[35]
$Ni/MgAlO_x$	17.2–57.8	2	250	12:3:5	2400 h^{-1}	97.9	97.5	[36]
$Ni/MgAlO_x$/SiC	12.5	5	400	4:1	60 L g_{cat}^{-1} h^{-1}	78.4	93.5	[37]
Ni–Fe/Al_2O_3	65–70	2	350	76:19:5	12 L g_{cat}^{-1} h^{-1}	96	>99	[38]
Ni–$Fe/MgAlO_x$	72.6	3	300	4:1	20 000 h^{-1}	83	97	[39]
Ni–Fe/Al_2O_3	39.6	≈1	250, 8	4:1:5	150 L g_{cat}^{-1} h^{-1}	≈45	>99	[40]
Ni–Mn/Al_2O_3	36.3	≈1	250, 8	4:1:5	150 L g_{cat}^{-1} h^{-1}	≈85	>99	[40]
Ni–Fe–Mn/Al_2O_3	35.6	≈1	250, 8	4:1:5	150 L g_{cat}^{-1} h^{-1}	≈80	>99	[41]
Ni–La/MgO	21	3	250	12:3:5	12 000 h^{-1}	56	>99	[42]
Ni/CeO_2–Al_2O_3	≈6	3.6	300	4:1	60 L g_{cat}^{-1} h^{-1}	≈75	>99	[43]
$NiCeZr/MgAlO_x$	20	3	375	4:1	20 000 h^{-1}	≈35	–	[44]

[a)]All reactions were run at atmospheric pressure; [b)]X_{CO2}—CO_2 conversion; [c)]S_{CH4}—selectivity of CH_4.

to achieve better crystallization, a higher surface area, and pore volume. With the aim to reduce the average particle size of Ni on Al_2O_3 support, Abelló et al. prepared Ni/Al_2O_3 HT precursors by coprecipitation at constant pH.[27] Although at high Ni loading (≈70 wt%), the Ni nanoparticles size in the range of 5–10 nm was achieved, demonstrating the advantage of using HT precursors. He et al. also reported a high-loading Ni/Al_2O_3 HT catalyst (78 wt%) with a very small Ni particle size in the range of 3–9 nm.[29] Despite different values of pH used during synthesis, HT-derived catalysts were successfully prepared with a homogeneous distribution of Ni on Al_2O_3 support.

In comparison with other conventional Ni/Al_2O_3 catalysts such as commercial catalysts and catalysts prepared by incipient wetness impregnation, Ni^{2+} surface species in HT-derived catalysts were harder to be reduced, reflecting a stronger metal–support interaction and a better metal dispersion.[28,29] The reducibility of Ni species was proportional to Al content, which could be explained by the formation of hardly reducible spinel $NiAl_2O_4$.[30] In fact, when only Ni and Al are incorporated in the LDH structure, it is called takovite and can be synthesized with Ni/Al molar ratios in the range of 1–5.6.[45] Gabrovska et al. found that this ratio could influence the crystallization degree of the precursors. A series of Ni/Al_2O_3 HT catalysts with varied Ni/Al molar ratios in the range of 0.5–3 was investigated.[30,31] The catalyst with a Ni/Al molar ratio of 2 exhibited the best performance in terms of CO_2 conversion and CH_4 selectivity. Notably, the catalyst maintained its activity during the 500 h long-term test at 275 °C. It is also noteworthy that a higher Ni/Al molar ratio did not significantly influence the catalytic performance of Ni/Al_2O_3 HT catalysts.[32] For instance, the CO_2 conversion of catalysts with a Ni/Al molar ratio of 3, 4, and 5 was 85–88%, whereas CH_4 selectivity was always ≈100% at 300 °C [gas hourly space velocity (GHSV) = 2400 h^{-1}, $H_2/CO_2 = 4$]. Moreover, mechanistic insights based on in situ Fourier transform infrared spectroscopy (FTIR) analysis during methanation reaction were provided.[31,32] Formate species as intermediates were detected, and the reaction mechanism via the formate pathway was proposed. In addition, the kinetic rate expression was important for the design of a full-scale methanation reactor. A kinetic study was also conducted for CO_2 methanation over Ni/Al_2O_3 HT catalysts, from the power law to the Langmuir–Hinshelwood approach.[33]

Overall, HT-derived catalysts exhibited better performance than conventional catalysts in CO_2 methanation. The Ni/Al_2O_3 HT catalyst (Ni/Al = 5, 70 wt% Ni) was able to maintain a high selectivity toward CH_4 (>99.7%) for 350 h of CO_2 methanation at harsh conditions (400 °C, 10 bar), even though the CO_2 conversion slowly decreased from 92.4% to 83.5%.[27] In fact, it was reported that Ni/Al_2O_3 HT-derived catalysts had better stability than conventionally impregnated catalysts, although slight deactivation was observed.[46] Abate et al. also concluded that Ni/Al_2O_3 HT-derived catalysts showed a more satisfactory stability and higher performance than commercial Ni/Al_2O_3 catalysts (at 300 °C and GHSV = 20 000 h^{-1}).[28]

2.2. Promoted Ni-Based HT-Derived Catalysts

The introduction of alkaline-Earth species to strengthen the surface basicity has been widely recognized as an effective way to improve catalytic activity and stability.[47] Studies on CO_2 methanation with promoted HT-derived Ni catalysts are also shown in Table 1. Liu et al. prepared the Ni nanocatalyst supported on Mg/Al mixed metal oxides derived from HT precursors.[36] Although the density of Ni nanoparticles increased as a result of a high Ni/Mg molar ratio, their average size remained the same at ≈2.5 nm. Compared with conventional Ni/Al_2O_3 and Ni/MgO catalysts, Ni/MgAl HT-derived catalysts showed better metal dispersion and significantly smaller particle size. Furthermore, the total basicity of the Ni/MgAl HT catalyst was enhanced, which was obviously due to the contribution of Mg species with medium-strong basic sites. As expected, Ni/MgAl HT catalysts (36.9 wt% Ni, (Ni+Mg)/Al = 2) exhibited an outstanding performance in CO_2 methanation, compared with Ni/Al_2O_3, Ni/MgO, and Ni/carbon nanotube (CNT) catalysts. The conversion of CO_2 reached 97.9% at 250 °C with diluted feed gases ($H_2/CO_2/Ar = 12/3/5$, GHSV = 2400 h^{-1}, 1 bar). The time-resolved diffuse reflectance infrared (IR) Fourier transform spectroscopy (DRIFTS) measurement was reported, suggesting that MgO could play an important role as an active site for CO_2 activation to form carbonate/hydrocarbonate species.

Bette et al. also prepared Ni/MgAl HT catalyst at the same (Ni + Mg)/Al molar ratio of 2 but at a higher Ni loading of 59 wt%.[34] In another work reported by Wierzbicki et al., the influence of Ni content of Ni/MgAl HT catalysts on the performance of CO_2 methanation was studied.[35] Apparently, the highest CO_2 conversion was achieved by the catalyst with the highest amount of Ni. The temperature-programmed reduction (TPR) study demonstrated that a large amount of Ni weakened the metal–support interaction and Ni species was easier to be reduced in Ni-rich catalysts. In contrast, the Ni-rich catalysts were found to have stronger basicity. The number of medium-strength basic sites increased steadily with the increase in Ni/Mg ratio when the M^{2+}/M^{3+} ratio was kept constant. Thus, the role of Mg was not clearly observed in this study, and Ni content was the dominating factor on the activity of Ni/MgAl HT catalyst. Nevertheless, Ni/MgAl HT-derived catalysts are considered as excellent alternatives for CO_2 methanation. An optimal tradeoff between H_2 activation (by Ni sites) and CO_2 activation (by basic sites of support) could be induced by a suitable composition of Ni, Mg, and Al. Hence, higher activity and stability could be achieved for CO_2 methanation, especially at low temperatures.

As mentioned, catalysts with good activity at low temperatures are highly desirable. An interesting concept was developed by Wang et al., who combined an HT-like structure with SiC substrate, known for high heat conductivity and superior thermal stability.[37] The Ni/MgAl–SiC catalysts exhibited better performance than Ni/MgAl HT catalysts, particularly at 275–300 °C, which could be ascribed to higher reducibility and a higher metallic surface area. A long-term test at 400 °C for 50 h showed that the Ni/MgAl–SiC catalysts had stable activity although slight deactivation still occurred, with CO_2 conversion dropping ≈1.5% over 50 h of reaction, which was assumed to be caused by mild metal sintering.[37] Another approach to increase the basic sites of support was reported by He et al., who fabricated the K–Ni/Al_2O_3 HT catalyst.[29] As expected, both the CO_2 conversion and CH_4 selectivity increased for the K-impregnated catalysts, which could be explained by the enhanced basicity from

the alkali metals. Comparisons in terms of enhancing the basicity between different types of alkali and alkaline Earth promoters are highly recommended.

A study on Ni–Fe/Al_2O_3 HT catalysts has been reported.[38] Fe was directly introduced into the HT structure during coprecipitation. The authors convinced that a certain amount of Fe addition could result in a catalytic system with a larger surface area, optimal particle size, and higher Ni dispersion. Using the Ni–Fe/Al_2O_3 HT catalyst (69 wt% Ni and 1.6 wt% Fe), the CO_2 conversion reached 80.8% at 219 °C but it was only 16.4% for the Ni/Al_2O_3 HT catalyst. Recent research suggested that Fe enhanced the adsorption of H_2 for CO_2 methanation,[48] whereas it is well known that the activity and selectivity of Fe catalysts are dependent on Fe loading and its oxidation state.[49] In fact, the bimetallic Ni–Fe catalyst was also considered as a promising candidate to substitute noble-metal catalysts in hydrogenation reactions.[50] Mebrahtu et al. studied the synergistic effect of bimetallic Ni–Fe alloys HT-derived catalysts for CO_2 methanation.[51] The addition of Fe increased the particle size, total basicity, and reducibility but reduced the surface area and total pore volume. It was found that Fe/Ni molar ratio of 0.1 was the best composition for Ni–Fe/MgAl HT catalyst (12 wt% Ni, $M^{2+}/M^{3+} = 3$). Both basicity and metal particle size were optimized at this ratio to accelerate the dissociation of H_2 from metallic sites and CO_x species from the support. The catalyst also exhibited a high stability in a 24 h long-term test without any observation of deactivation. However, the activity test was only conducted at 335 °C; thus, the challenge of CO_2 methanation at low temperatures was not pronounced. In another study, the authors further studied the deactivation of the bimetallic Ni–Fe catalysts during low-temperature CO_2 methanation.[39] They suggested that the formation of $Ni(OH)_2$ caused deactivation, which could be suppressed by doping Ni with Fe.

Apart from Fe, Mn has also been investigated as a promoter for CO_2 methanation, especially via HT-derived catalysts.[40] Mn as a promoter in Ni–Mn/Al HT catalysts appeared to improve the medium basic sites, which led to an increase in CO_2 adsorption. In contrast, the Fe promoter was assumed to strengthen the thermal stability of the catalysts. Hence, to increase the catalytic activity, a high amount of Mn addition was preferred, whereas a high amount of Fe was recommended to increase the stability. Indeed, the performance of Ni–Fe–Mn/Al HT-derived catalysts was significantly better than Ni/Al HT catalysts.[41]

Lanthanum has been shown to have a positive effect on CO_2 methanation. According to Wierzbicki et al., although La species existed as a separate phase and was not incorporated into the HT structure of Ni–La/MgAl HT catalyst (15 wt% Ni), La increased the total basicity due to its medium-strong basic sites.[42] Therefore, CO_2 adsorption capacity was enhanced. In this case, the catalyst with La loading of 2 wt% exhibited the highest CO_2 conversion and more significantly at a low temperature (<300 °C). The authors also studied the effect of different preparation methods of Ni–La/MgAl HT catalysts. Ion exchange using the La–ethylenediaminetetraacetic acid complex was reported as the most suitable method to dope La into the Ni/MgAl HT catalyst. The catalytic performance was very stable for the 24 h long-term test without any metal sintering or carbon deposition.

As mentioned earlier, Ce was one of the promising promoters to obtain highly active catalysts. Ni–Ce HT precursors were impregnated on γ-Al_2O_3 support by Xu et al.[43] Although the role of Ce addition was not addressed, this study revealed that the HT precursors that impregnated on Al_2O_3 support showed better catalytic performance than conventional catalysts. Interestingly, instead of using the traditional calcination method, the cold plasma technique was used to improve the catalytic properties. Moreover, cold plasma via dielectric barrier discharge (DBD) technology can also be implemented on the traditional fixed-bed reactor. Ni–Ce–Zr/Mg–Al HT catalysts presented the higher CO_2 conversion of ≈70% at 325 °C in CO_2 methanation using plasma, compared with the conventional reactor, where merely 5% of CO_2 conversion was achieved at similar conditions.[44]

3. Structured Catalysts and Reactors

Fixed-bed reactors, i.e., packed-bed reactors, are commonly used for CO_2 methanation due to their simplicity and cost effectiveness. The reactors provide more contact between the reactant gases and the catalyst granules/pellets. However, random maldistribution in the fixed-bed reactors causes nonuniform access of reactant gases to the catalytic surface, unexpected hotspot, and thermal runaways of exothermic reactions, which are the most challenging problems of the methanation process. The overall process performance, CH_4 yield, CH_4 selectivity, and the lifetime of the catalysts are consequently reduced. Therefore, different reactor concepts focusing on heat management have been proposed.[52] One of the most common reactor concepts with intensified heat transfer is structured reactors equipped with well-designed structured catalysts. The hydrodynamics in a structured reactor can be simplified as uniform laminar flow, enabling full access of reactant gases to the catalytic surface with a lower pressure drop and possibly diminishing mass transfer limitations.[53] Structured catalysts with high thermal conductivities could also increase the overall heat transfer coefficient, thus improving the heat transfer performance of the reactor.[54] For instance, based on modeling studies, Schlereth et al. concluded that honeycomb monolith reactors have superior performance in comparison with fixed-bed reactors in terms of heat transfer efficiency, although it was only applied on specific operating conditions of CO_2 methanation.[55]

In general, structured catalysts consist of a 3D-shaped support with a layer of catalytic material. The support materials are ceramic type (e.g., Al_2O_3, cordierite-Al_2O_3, MgO, SiO_2, SiC, etc.), metallic type (e.g., Al, Ni, Cu, Co, stainless steel, Inconel, FeCrAlloy, etc.), or carbon-type (e.g., activated carbon, reticulated vitreous carbon). Several 3D structural configurations are honeycomb, corrugated sheet, gauze, foam, fiber, wire packing, or periodic open-cellular structures.[56] Although the use of structured catalysts and reactors has been discussed in a previous study,[57] we present a more systematic and detailed review of the recent developments of conventional structured catalysts for CO_2 methanation, together with the latest innovative concepts of catalyst manufacturing. A summary of different configurations of structured catalysts and reactors applied for CO_2 methanation is shown in **Table 2**.

Table 2. Summary of structured catalysts and reactors for CO_2 methanation.

Structured catalyst types	Catalysts	Reactor type	Ref.
Cordierite honeycomb monolith (400 cpsi)[a)]	$Ru/\gamma\text{-}Al_2O_3$	Fixed bed	[58]
Aluminum honeycomb fin (45 × Ø18 mm, 100–200 cpsi)	Ni/CeO_2	Conventional flow type	[59,60]
Cordierite monolith (15×Ø10 mm, 500 cpsi)	Ni/gadolinium-doped-ceria (GDC)	Fixed-bed quartz tubular	[61]
Cordierite honeycomb square channel (50 × 50 × 142 mm, 300 cpsi)	$Ni/\gamma\text{-}Al_2O_3$	Innovative single-stage lab scaled	[62]
Aluminum and stainless steel honeycomb (100 × Ø80 mm)	Ni/Al_2O_3	Multitube fixed bed (heat exchange by oil)	[63]
Ceramic honeycomb with square cell structure (100–300 cpsi)	Ni/CeO_2	Fixed-bed quartz tubular	[64]
SiC foam (150 × Ø20 mm)	Ru/TiO_2	Fixed bed	[65]
Ni foam (Ø16 mm)	Ni/Al_2O_3	Fixed-bed quartz tubular	[66]
Sponge Ni	–	Fixed-bed quartz tubular	[67]
SiC, aluminum, and alumina open-cell foam	$Ni\text{-}Ru/CeO_2\text{–}ZrO_2\text{–}CNF$	PMR and double-walled reactor exchanger	[68–71]
Aluminum open-cell foam	Ni/Al_2O_3	Metallic foam reactor channel (heat exchange by oil)	[72]
Aluminum open-cell foam and SiC honeycomb monolith (150 cpsi)	$Ni/CeO_2\text{–}ZrO_2$	Fixed-bed quartz tubular	[73]
Spiral aluminum plate	Ni/CeO_2	Fixed-bed quartz tubular	[74]
FeCrAlloy plate	Ni/Al_2O_3	Plate reactor	[75,76]

[a)]cpsi—cells per square inch.

3.1. Honeycomb Monolith Catalysts and Reactors

One of the early studies using monolithic catalysts for methanation was conducted by Jarvi et al.[77] The authors reported that the monolithic-supported Ni catalyst was significantly more active and selective in CO methanation compared with catalysts in bead and pellet forms. Because of superior performance with a low-pressure drop at high space velocities, the honeycomb Ni-based catalysts were recommended as ideal catalysts for high throughput methanation. Despite those initial promising findings, the industrial applications of structured reactors were scarce and limited until the past decade, particularly for CO and CO_2 methanation. In recent years, there has been a considerable number of research using structured catalysts, particularly honeycomb monoliths for the synthesis of CH_4 from CO_2 and H_2.

The application of monoliths for CO_2 methanation was first introduced as a model for heat exchanger by Janke et al.[58] Although the reaction was conducted at low space velocity, the $Ru/\gamma\text{-}Al_2O_3$ monolith catalyst exhibited excellent activity at very low temperatures of CO_2 methanation (200–250 °C). Repeated tests on the spent monolith were also conducted and showed nearly the same activity as that of the fresh one. This is one of the earliest studies which proved the feasibility of wash-coated honeycomb monoliths for CO_2 methanation.

Recently, a honeycomb-structured catalyst with a high CO_2 methanation performance was reported by Fukuhara et al.[59] Among different support materials (i.e., Al_2O_3, ZrO_2, CeO_2, TiO_2, Y_2O_3, and MgO), CeO_2 was identified as the best catalyst with the highest activity in CO_2 methanation. The Ni/CeO_2 catalyst was subsequently wash coated on an Al substrate with different honeycomb-fin configurations. A temperature spike of ≈20 K from the set temperature was observed in the granular-type catalytic bed during reaction. In contrast, it was confirmed that the temperature of the honeycomb-type catalytic bed was constant and close to the set temperature. The advantage of structured reactors using monolith catalysts in terms of heat exchange and hotspots prevention was recognized.

The authors further investigated different stacking strategies of honeycomb monoliths and developed a multistacked design (**Figure 2**). For segment-type configuration, the optimum 15 mm-gap distance was found to boost the performance of catalysts.[60] Coated catalysts were placed alternating with static mixers which were considered as an advanced part to accelerate the mass transfer.[78] Even though hotspots were observed during reaction, the random flow channel and gap distance enhanced the methanation performance at low temperatures and high flow rate without pressure drop. The catalyst stability was maintained at a high CO_2 conversion of 92.7% with a slight decrease of 0.6% over 76 h at 300 °C and a highly undiluted flow of 3 L min^{-1}. The metallic honeycomb catalyst in multistacked design revealed an extremely promising concept for CO_2 methanation.

Cordierite, or magnesium iron aluminum cyclosilicate, is a common ceramic-type material used in monoliths manufacturing. Vita et al. used this type of substrate to enhance the activity of Ni-based catalysts (**Figure 3**a).[61] However, instead of using the conventional wash-coating method, the authors used solution combustion synthesis to prepare the structured catalysts. Solution combustion synthesis was suggested as a suitable procedure to deposit thin, adhesive, and uniform catalytic layers on the ceramic surface.[79] The monolith system showed better activity than the powder-type catalysts in terms of CH_4 productivity. A long-term reaction test was conducted at 400 °C and GHSV of 30 000 h^{-1}. During the reaction, the temperature at the center and outlet of the catalytic bed plunged up to 476 and 448 °C, respectively. Despite hotspot formation, the ceramic-type monolith still maintained its high activity with CO_2 conversion of 68–69% throughout 200 h of reaction.

Ahn et al. pointed out the knowledge gap in the influence of coating materials on the catalytic performance of honeycomb catalysts.[64] The authors used industrial ceramic honeycomb

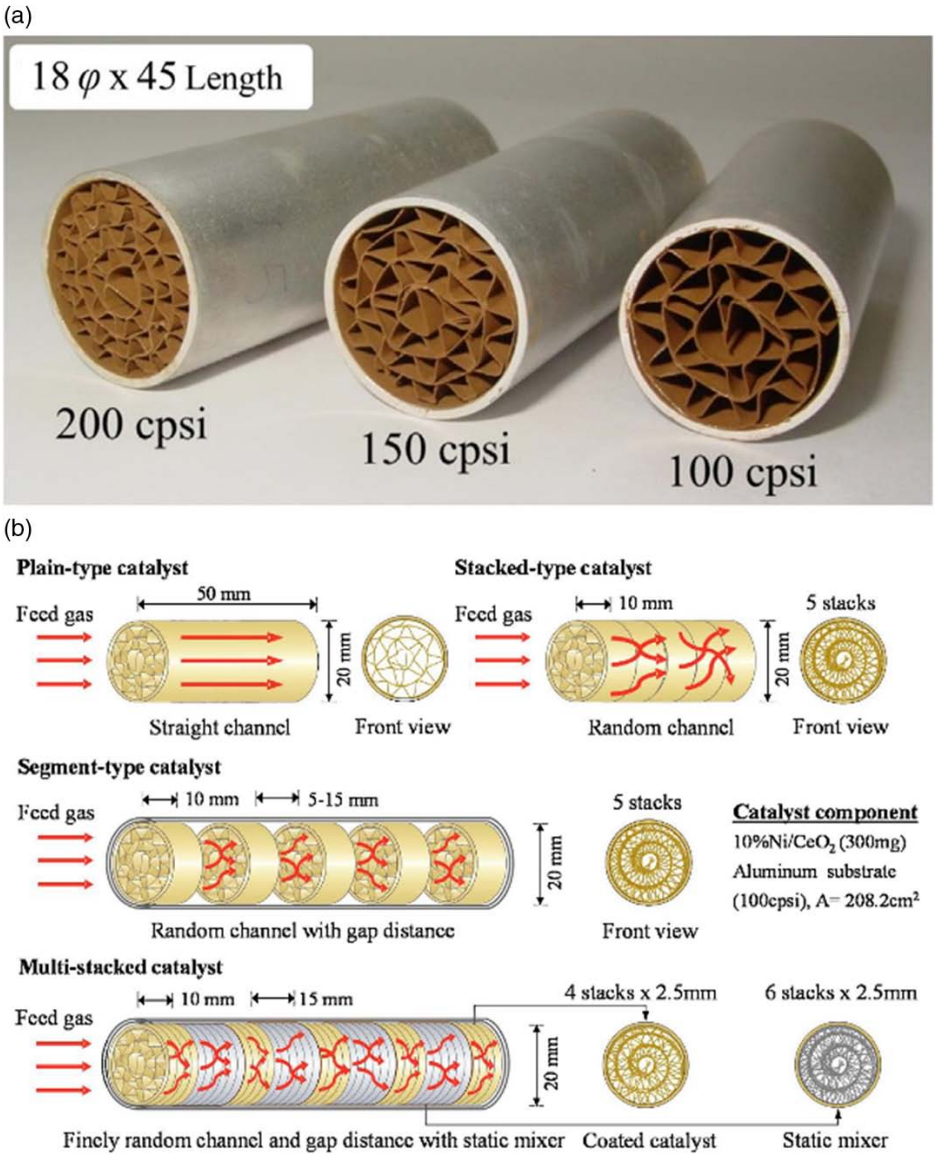

Figure 2. a) Overview of Al-honeycomb Ni-based catalysts with different cell density. Reproduced with permission.[59] Copyright 2017, Elsevier. b) Different configurations of the honeycomb catalysts: plain, stacked, segment and multi-stacked types. Reproduced with permission.[60] Copyright 2018, Elsevier.

support with various cell densities. Isopropanol was reported to be the most suitable coating liquid to achieve high CO_2 conversion, regardless of concentration. The excellent activity of Ni/CeO_2 powder-type catalyst was reconfirmed among Ni/Al_2O_3, Ni/Y_2O_3, and Ni/TiO_2 catalysts. The material was subsequently used to prepare honeycomb-type catalysts (Figure 3b). The square honeycomb catalyst at a higher cell density exhibited better performance, particularly at the low-temperature region, which could be ascribed to the higher surface area of the catalyst.

Many efforts have been dedicated to the innovation of the conventional fixed-bed reactors. A multibed reactor with up to four chambers per stage was proposed by Biegger et al.[62] The authors first tested two single-stage lab-scaled reactors using a square honeycomb $Ni/\gamma\text{-}Al_2O_3$ catalyst. CH_4 productivity achieved in the second reactor was significantly higher than the first reactor, as expected. Although heat management was not successfully achieved in this work, the possibility of enhanced CH_4 production via a multistage reactor system was revealed.

By mathematical modeling, a honeycomb reactor was simulated and upgraded to a semicommercial scale by Schollenberger et al.[63] The authors aimed to optimize the reaction path with a high reaction rate. The mathematical model was successfully developed and experimentally validated with commercial honeycomb Ni/Al_2O_3 catalysts. To obtain products with more than 95 vol% of CH_4, a reactor with two reaction zones was suggested. It was assumed that the high-temperature gas inlet was kinetically controlled and had a maximum possible rate, whereas the low-temperature gas outlet was controlled by thermodynamics and adjusted the necessary equilibrium composition. Based on the experimental temperature profiles and

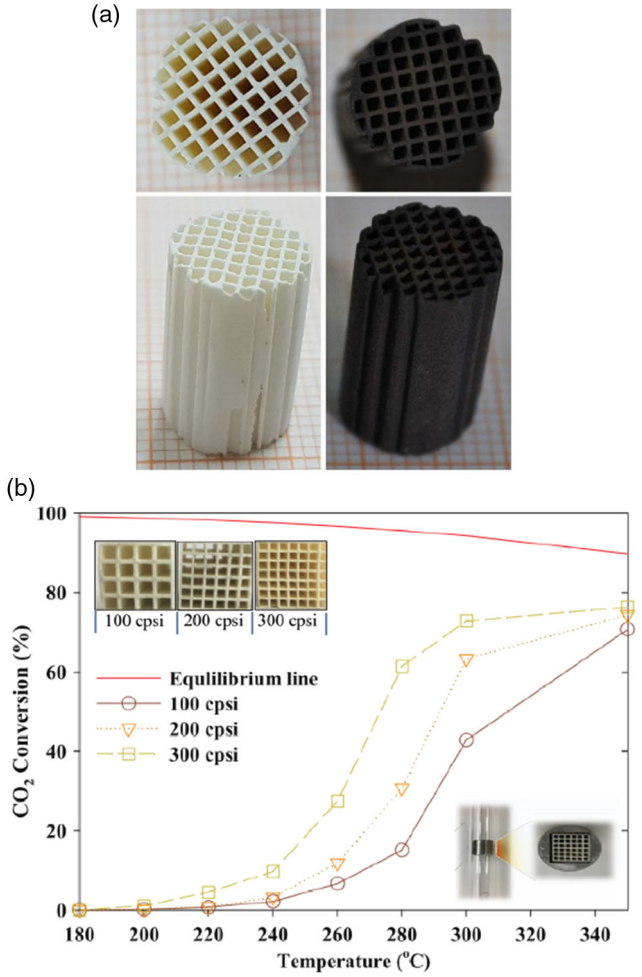

Figure 3. a) Photographs of uncoated (left) and coated (right) cordierite monoliths. Reproduced with permission.[61] Copyright 2018, Elsevier. b) CO_2 conversion in CO_2 methanation over 10 wt% Ni/CeO_2 honeycomb-type catalysts at different cell densities. The image of the honeycomb-type catalyst inside the quartz tube reactor is presented on the bottom right corner. Reproduced with permission.[64] Copyright 2019, Elsevier.

specific production rates, the combination of aluminum and steel honeycomb was found to be the most promising design.

3.2. Foam-Type Structured Catalysts and Reactors

As mentioned earlier, the Sabatier process is very appealing for aerospace exploration missions. Shima et al. reported Ru/TiO_2 on SiC foam catalysts for methanation reaction, which was a part of practical space systems called closed-loop air revitalization.[65] Later on, $Ni–Al_2O_3$ was embedded on Ni foam by the wet chemical etching method. While Ni foam could convert only 10% of CO_2 at 300 °C, a significantly high conversion of 91% could be achieved by $Ni–Al_2O_3$/Ni foam.[66] The improved heat transfer of foam-based catalysts was investigated by both experimental works and computational fluid dynamic (CFD) modeling. With an equivalent amount of reaction heat released from the catalytic surfaces at equal conversion, the foam-based catalytic bed generated a hotspot with ≈30 K temperature rise, whereas it was ≈155 K for the powder-packed bed. Hence, the exceptionally stable CO_2 methanation performance (CO_2 conversion of ≈90%, CH_4 selectivity of >99.9%) was observed during a 1200 h reaction over the foam-type catalyst at 320 °C. Ni foam was also reported as Ni sponge by Tada et al.[67]

Foam-based catalysts started to gain more attention in the application of small-sized structured reactors for the Sabatier reaction. A so-called platelet millireactor (PMR), with one single channel (**Figure 4**a), was used by Frey et al.[68] In their study, the central channel of the PMR contained β-SiC foam, which was impregnated with Ni–Ru-based catalysts. Based on specific CH_4 productivity, $Ni–Ru/CeO_2–ZrO_2$ powder catalysts showed superior performance to other catalysts. Interestingly, when carbon nanofibers (CNFs) were added to $CeO_2–ZrO_2$ support, the new foam-based catalysts ultimately exhibited better productivity. Moreover, for the first time, an in situ observation was conducted to study the reaction ignition and hotspot formation. The temperature on the foam surface during the methanation reaction was recorded by the IR camera (Figure 4b). The presence of the hotspot could be correlated with CH_4 and CO selectivity. Local hotspots were suspected to favor the reverse water gas shift (RWGS) reaction, which increased CO selectivity and reduced the CH_4 selectivity. However, the addition of CNFs allowing better heat transfer could be a good solution for the design of catalysts. Further investigation on the role of CNFs on foam catalysts is greatly appealing.[69]

Another study by Frey et al. revealed that SiC foam was a better support than Al and Al_2O_3 open-cell foam due to better anchoring strength.[70] Nevertheless, $Ni/CeO_2–ZrO_2$ coated on Al open-cell foam has been extensively tested.[71] A double-walled reactor exchanger was used for CO_2 methanation. Eight coated cylindrical foams (3 × ∅2 cm) were installed inside the reactor chamber. The foam had a central channel of 2 mm, allowing the insertion of a multipoint thermocouple, which can measure the temperature at six different positions. The experiments successfully proved that the hotspots are formed based on the temperature profiles along the reactor. More heat was released in the first one-third of the catalytic bed where a maximum temperature increase of 25 K was measured. Similarly, it was reported that at the higher set temperature, the Sabatier reaction released more exothermic heat, resulting in higher CH_4 productivity and CO_2 conversion. Subsequently, more severe hotspots were also suspected due to the high-temperature elevation.[66] Foam-structured materials were assumed to have excellent heat evacuation capacity, lower risk of thermal runaway, and premature catalyst deactivation, whereas the reactor exchanger was suggested to have advantages on heat convection. In this study, the heat transfer fluid was circulated outside the reactor tube at a maximum temperature of 320 °C. This could explain the temperature increase of only 25 K, when it could plunge up to 200–250 K in a powder-packed bed reactor under similar conditions.[80] The excellent heat transfer efficiency of the reactor exchanger can be useful for the development of the methanation reactor.

Bengaouer et al. evaluated the performance of the annular fixed bed, millistructured reactor channel, and open-cell foam reactor (i.e., metallic foam reactor channel).[72] The same commercial Ni/Al_2O_3 catalyst was used for comparison. Coated cellular Al open-foam pellets were stacked inside the foam

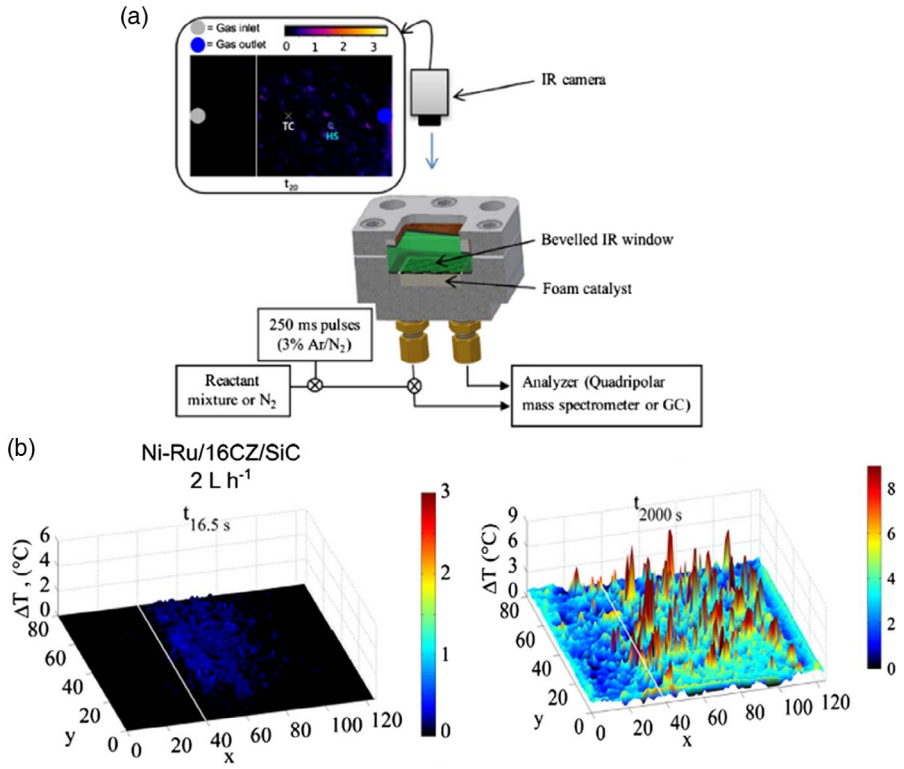

Figure 4. a) Simplified schematic of reaction set up, where foam-type catalyst was located inside a PMR equipped with an IR thermal camera; b) IR thermograph presenting ignition and stationary stage ($t_{16.5s}$ and t_{2000s}) of Ni–Ru/CeO_2–ZrO_2/SiC foam structured catalyst. Reproduced with permission.[69] Copyright 2019, Elsevier.

reactor. CH_4 yield, space–time yield, mass productivity, volumetric productivity, and temperature elevation were essential indicators for the reactor performance. Millistructured reactor channel exhibited the best volumetric productivity and space–time yield, although significantly the high-temperature elevation indicated poor heat management. In contrast, the metallic foam reactor showed excellent mass productivity and negligible hotspot formation, but the CH_4 yield was moderate. Thus, the authors proposed an alternative solution, such that two concepts could be combined for higher productivity and better thermal management.

As there are different configurations of structured catalysts, the comparison between monolith and foam type, for instance, is interestingly necessary. Ricca et al. tested the 5 wt% Ni/CeO_2–ZrO_2-supported catalysts in both powder and structured forms.[73] Based on adhesion tests, Al foam seemed to have less anchoring strength than SiC monolith. At 300 °C, the catalyst on SiC monolith achieved the highest CO_2 conversion and CH_4 selectivity. Undesirable hotspot formation was detected in all catalytic beds according to the thermal profiles. Although a temperature elevation of 100 K was measured, the heat dissipation on the SiC monolith bed was better than that of Al foam and powder bed.

3.3. Other Types of Structured Catalysts and Reactors

A spiral-type Ni/CeO_2 catalyst was prepared by Fukuhara et al.[74] The structured substrate was the Al plate, twisted to form the spiral shape, and subsequently wash coated by a slurry granular of Ni/CeO_2 catalyst. CO_2 conversion of 50% was obtained at a low temperature of ≈280 °C at GHSV of 80 L g_{cat}^{-1} h^{-1}, demonstrating the outstanding activity of the catalyst in CO_2 methanation. Moreover, an automethanation process (i.e., $CO_2 + 6H_2 + O_2 \rightarrow CH_4 + 4H_2O$) was also reported. The reaction readily occurred at room temperature, and ≈60% CO_2 was converted by the same catalytic system. An IR thermal image was recorded (**Figure 5**). The extremely exothermic heat released was clearly seen near the inlet of the reactor during reaction at room temperature. Despite a huge temperature spike of ≈300 K, the structured catalyst was able to maintain its stable activity during the 60 h test.

3.4. 3D Printing Structured Catalysts

In the past few years, an innovative technology developed from additive manufacturing, named 3D fiber deposition (3DFD), was used to produce macrostructured catalytic supports. 3DFD materials were constructed by the extrusion of a highly viscous paste consisting of metallic or ceramic mixtures through a thin nozzle. The so-called 3D printing catalysts provide better heat and mass transfer and lower pressure drops, for instance, similar to structured catalysts. However, the flexible design is the most significant feature.

Danaci et al. prepared stainless steel and copper support (3D-SS and 3D-Cu, respectively) using the extrusion method (**Figure 6**).[81,82] The support was then dip coated with

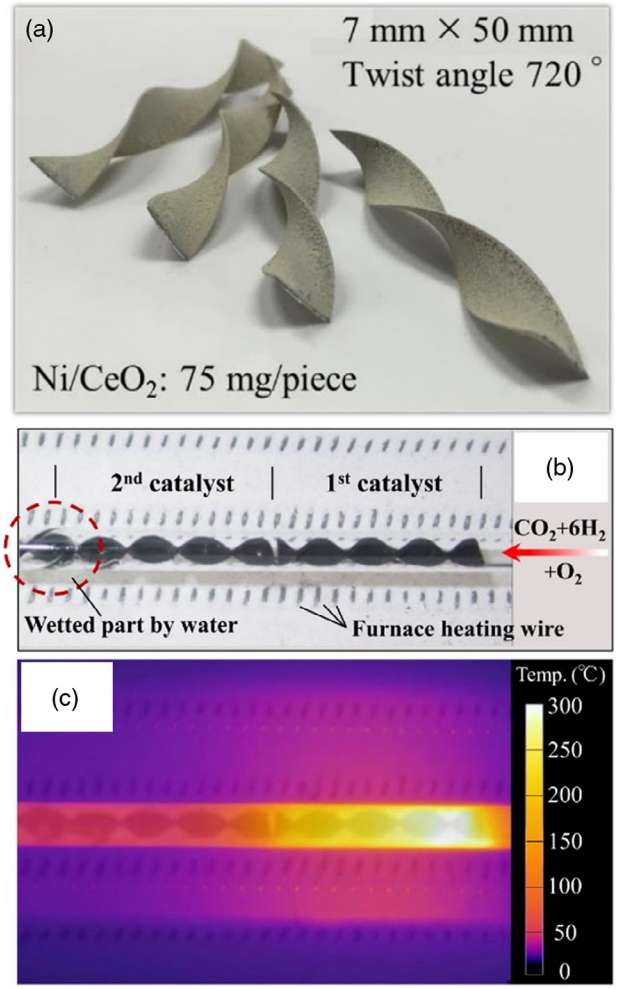

Figure 5. a,b) Coated spiral plate-type catalysts in the quartz reactor tube and c) snapshot of IR thermal image during the automethanation reaction at room temperature. Reproduced with permission.[74] Copyright 2019, The Chemical Society of Japan.

Ni/alumina suspension, dried, and sintered to form 3DFD structured catalysts. The challenge of homogeneous coating is addressed in this study, and optimal compositions for coating suspension were proposed. Indeed, the 3DFD catalysts showed better CO_2 conversion than the powder-type catalysts, even though only at high temperatures above 300 °C. Scaled-up experiments were investigated in a mini-pilot reactor with stacked 3DFD structured catalysts.[83] The authors successfully convinced the feasibility of CH_4 production using Ni/γ-Al_2O_3 catalysts on 3D-SS support. No hotspot formation was observed, which could be due to better heat transfer by the 3D catalytic network and/or by the circulated thermal oil.

The 3DFD method can be used to directly print out structured catalysts from the catalytic materials. Recently, Middelkoop et al. conducted 3D printing of Ni/Al_2O_3 structured catalysts in tetragonal shape.[84] A well-developed homogeneous ink was prepared and extruded through a nozzle of a syringe (**Figure 7**), whereas its position was computationally controlled.[85] The ink/paste consisted of catalytic materials in fine powder form and the binders.

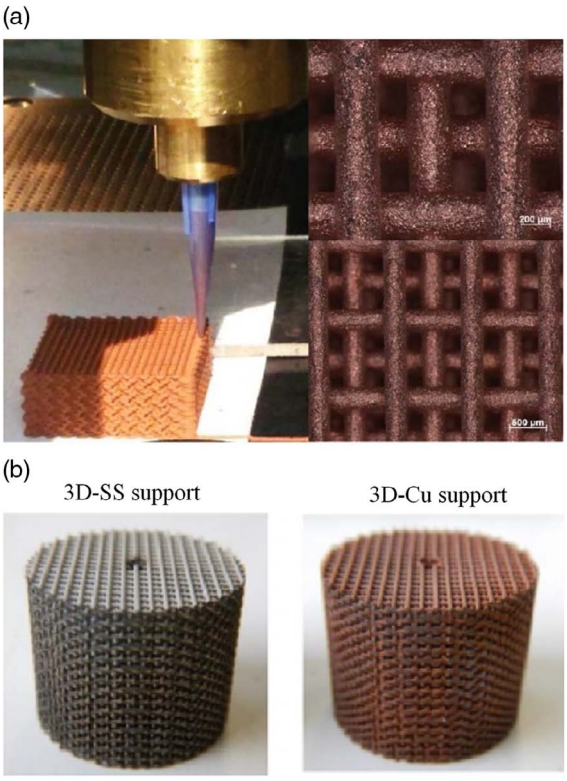

Figure 6. a) 3DFD manufactured by extrusion of copper supports and its optical microscope images. b) The 3D-printed supports made of stainless steel and copper. Reproduced with permission.[82] Copyright 2018, Elsevier.

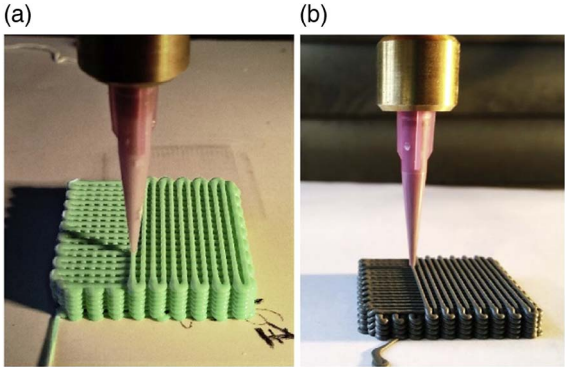

Figure 7. Tetragonal structured catalysts prepared by 3D printing. The catalytic phase in the printing ink/paste was a) as-prepared Ni alumina and b) commercial Ni alumina. Reproduced with permission.[84] Copyright 2019, Elsevier.

The binders were a mixture of polymer (e.g., methylcellulose), water, inorganic binders (e.g., colloidal silica and bentonite), and additives to achieve desired and reproducible rheological properties. The finished products were dried and subsequently heat treated at 500 °C to remove organic binders. The results showed that directly 3D printing Ni/Al_2O_3 catalyst exhibited better activity in CO_2 methanation, compared with the conventional impregnated catalysts.

3.5. Microchannel Reactors

The small volume and reduced dimension of the reaction zone are typical features of the microchannel reactor. In contrast, microchannel reactors can also be considered as structured reactors, because the catalytic materials are usually impregnated on a metallic plate installed inside the channel. The reactor enables more facile process control and thermal management for catalytic reactions at high temperatures.[86] Moreover, the improvement of hydrodynamics in the reaction zone can prevent the formation of hotspots and consequently the deactivation of catalysts. Nevertheless, microchannel reactors still have some drawbacks, e.g., a one-time-used system and limited scaling-up ability which prevent it from industrial applications. Many researchers have applied microchannel reactors for the development of the Sabatier process or PtG technology.

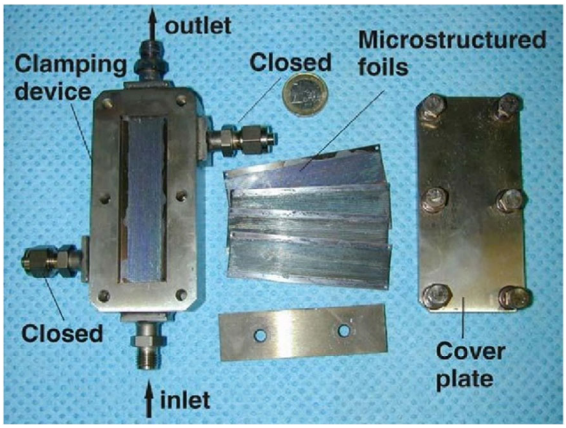

Figure 8. Microchannel reactor with clamping device and coated microstructured foils. Reproduced with permission.[87] Copyright 2005, Elsevier.

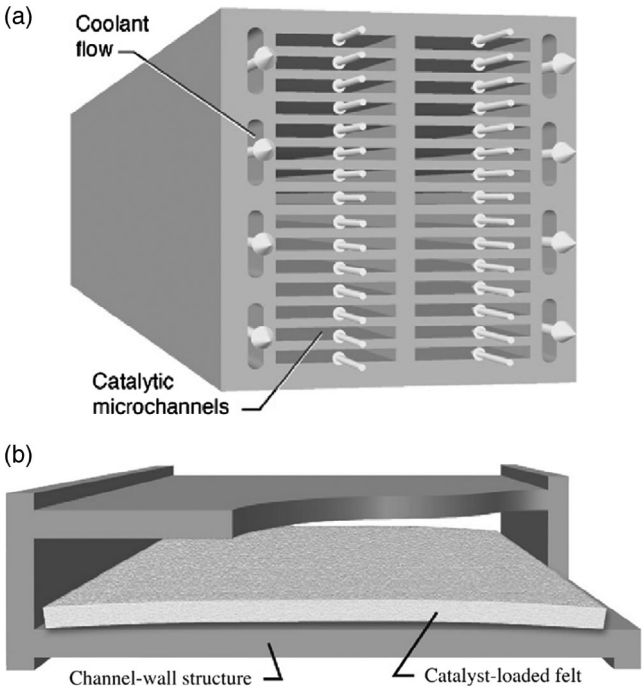

Figure 9. a) Illustration of a section of the microchannel reactor and b) a single channel with an interior coated metal felt. Reproduced with permission.[89] Copyright 2007, Elsevier.

Görke et al. first reported a highly selective methanation process using microchannel reactors coated with Ru/SiO_2 and Ru/Al_2O_3 catalysts.[87] The reactors consist of stainless steel foils with etched microchannels, which were coated with Al_2O_3 or SiO_2 gel (**Figure 8**). After calcination, Ru was impregnated on the coated foils. Although the work focused on CO methanation, CO_2 methanation was also tested at a temperature range of 100–380 °C with a highly diluted gas ($H_2/CO_2/N_2 = 25/4.5/70.5$). It was found that the Ru/SiO_2 catalyst exhibited good performance with high CH_4 yield at a low temperature of 170 °C. The temperature was assumed to be easily controlled with precision due to small dimensions and the enhanced heat transfer efficiency of the microreactor systems.

The microchannel designs were further investigated for applications such as propellant production on Mars or space habitat air revitalization. Prior to studying the microchannel reactor, Hu et al. evaluated many catalysts and supports in a packed-bed reactor.[88] The felts made of FeCrAlY intermetallic alloy were coated with 3 wt% Ru/TiO_2 catalyst and subsequently installed inside the single-channel reactor. The CO_2 conversion

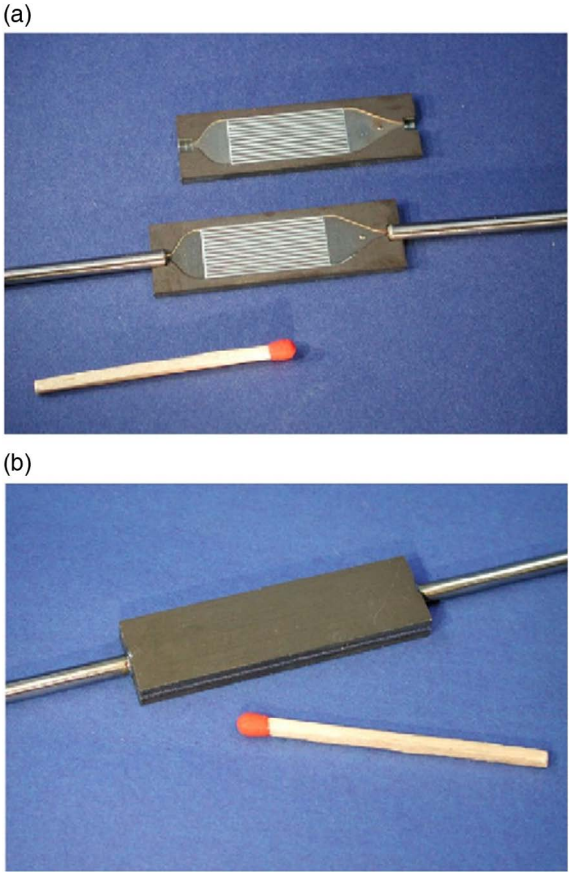

Figure 10. Sandwiched microchannel reactor: a) coated platelets with capillary and b) laser-welded reactor. Reproduced with permission.[90] Copyright 2007, Elsevier.

reached 78.6% at 365 °C (GHSV = 30 500 h^{-1}), even after the reactor was shut down and restarted during repeated tests.

Hu and coworkers continued the research on the challenging multichannel reactors. The microreactor with two parallel columns of 15 microchannels each was fabricated (**Figure 9**a).[89] More importantly, the felt was not directly bonded to the channel walls but separately inserted into the channels (Figure 9b). This method could overcome the disadvantageous "single-use" factor when applying microchannel reactors for any catalytic process. To avoid the initial temperature spike during the exothermic reaction, a short catalytic heat-exchanger section was designed, limiting the temperature increase up to 350 °C. Without this part, the initial temperature could increase up to 650 °C, potentially causing damage for catalysts.

Another microchannel reactor design was reported by Men et al. for both CO and CO_2 methanation.[90] The reactor had a sandwich design with two face-to-face microstructured platelets attached together. One pair of platelets with 14 channels containing coated catalysts was sealed by laser welding, together with the inlet and outlet capillaries (**Figure 10**). In this study, the Ni/CaO–Al_2O_3 catalyst was found to be the best catalytic system for CO_2 methanation at a low temperature of 200 °C. The designed microchannel reactor was considered as an excellent tool to investigate the reaction kinetics by tuning the feed compositions and reaction temperature.

Although the coated metallic substrate inside the microchannel was beneficial in terms of low-pressure drop, potential adhesion failure can occur, and catalytic layers could detach from the metallic substrate during the reaction due to differences in thermal expansion coefficients. An excellent metal–ceramic complex substrate with good stability was developed by Liu et al. (**Figure 11**).[91] The FeCrAlloy substrate was sprayed with a layer of Al_2O_3, heated to 1200 °C to ensure the embedding, further deposited with AlOOH sol, and subsequently impregnated with Ni ions. The results of the vibration test showed a minor weight loss, implying the potential of using metal–ceramics complex substrate in microchannel reactors for further process development.

Recently, Engelbrecht et al. developed a CFD model of microchannel reactors for CO_2 methanation.[92] The kinetic parameters of both Sabatier and RWGS reactions were estimated and validated by experimental data. The commercial Ru–Cs/Al_2O_3 catalysts were wash coated on 80 microchannels in the microreactor. The reactor (**Figure 12**) achieved 83.4% of CO_2 conversion at 400 °C and 5 bar with a high gas flow rate of 97.8 L g^{-1} h^{-1}. This high performance could be maintained for 150 h on stream, indicating an excellent stability of the catalytic system. The latest research on CO_2 methanation over Ni-based coated on the FeCrAlloy plate in a single-channel reactor (**Figure 13**a) was reported by Lalinde et al.[75,76] Different formulae of coating slurry and coating methods (i.e., brush coating, spin coating, and frame coating) were considered for the coating process optimization. For the first time, the thickness of the coating layer was measured by a profilometer. The nearly

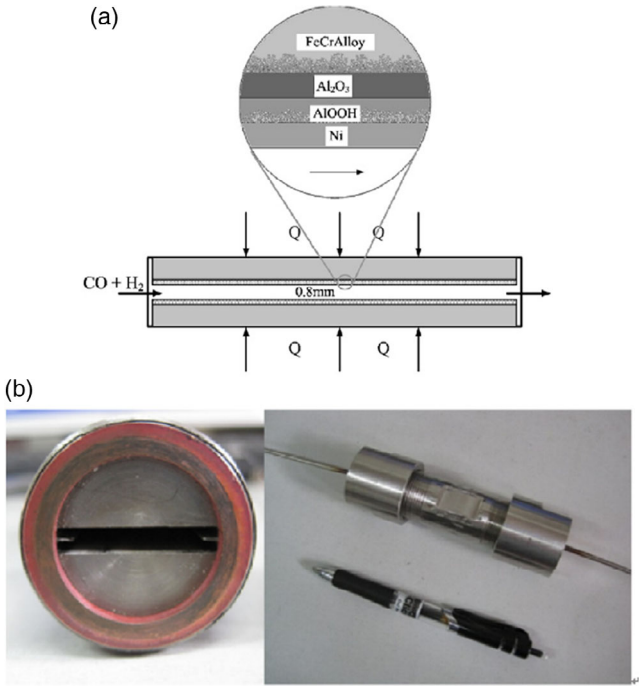

Figure 11. a) Schematic diagrams of metal–ceramics complex substrate with catalyst loading. b) Images of the microchannel reactor. Reproduced with permission.[91] Copyright 2012, Elsevier.

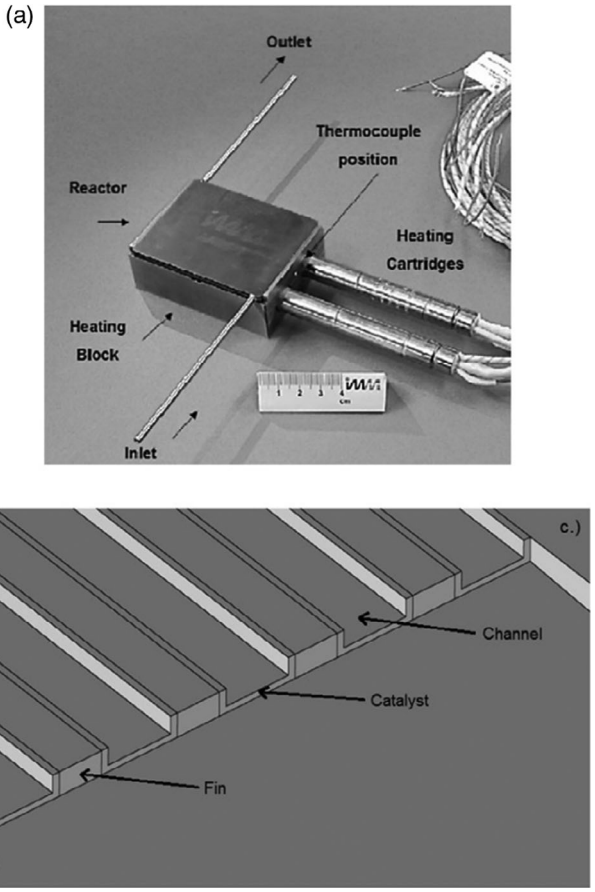

Figure 12. a) Reactor with laser-welded inlet/outlet tubes, heating block, and electric heater cartridges. Reproduced with permission.[93] Copyright 2015, Elsevier. b) Illustration of microchannels with the wash-coated catalyst. Reproduced with permission.[92] Copyright 2017, Elsevier.

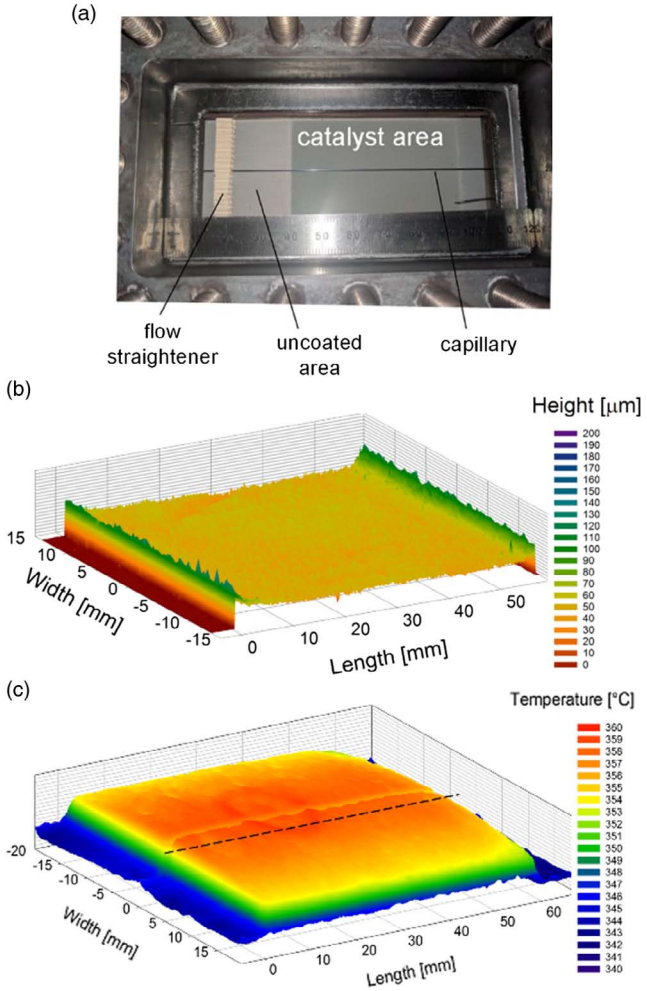

Figure 13. a) Catalytic plate reactor with the effective channel ($5 \times 40 \times 100$ mm). b) 3D catalyst height profile, measured by profilometer. c) 3D surface temperature profile during CO_2 methanation. Reproduced with permission.[75] Copyright 2019, Elsevier.

homogeneous coating layers with a thickness of 40–60 mm in a flat area were observed (Figure 13b). It was concluded that the catalytic mass was better distributed by the frame coating method. Moreover, a 3D surface temperature profile of the plate channel reactor during reaction was also recorded (Figure 13c). The temperature elevation was assumed to be negligible, and no hotspot formation was detected.

4. Summary and Outlook

Considerable efforts have been made in the development of the catalytic systems and reactors for the Sabatier process. Regarding the discovery of new material as heterogeneous catalysts for CO_2 methanation, this Review has focused on the potential of HT materials as precursors for supported catalysts. HT-derived catalysts can be prepared via a simple and highly reproducible coprecipitation method. The material offers strong metal–support interaction and high dispersion of active sites. Many studies have shown that HT-derived Ni-based catalysts exhibited better catalytic activity and stability than that of conventional catalysts. Moreover, to improve catalyticactivity and stability for low-temperature CO_2 methanation, the addition of promoters with different purposes (e.g., as second active site, improved basicity, enhanced CO_2 and H_2 adsorption, etc.) or further advanced treatment (e.g., cold plasma technology) is feasible to be applied for HT-derived catalysts.

The implementation of laboratory research into industrial practice is usually conducted on structured catalysts and reactors as it provides better heat and mass transfer, enhanced hydrodynamics, etc. Structured catalysts have been intensively studied for CO_2 methanation in terms of different materials, configurations, and preparation methods. High CO_2 conversion and CH_4 yield at low temperatures could be achieved using structured catalysts. The structural reactor–exchanger concept with excellent efficiency in heat management is highly recommended to prevent hotspots' formation.

The latest catalytic preparations using additive manufacturing technology, such as 3D printing, have also been applied to obtain structured catalysts for the Sabatier reaction. Although, in an early stage, the application of 3D printing is promising for the future of chemical engineering and catalysis manufacturing. It enables a feasible fabrication of complex and geometrically customized catalytic design. Furthermore, both structured catalysts and structured reactors can be produced by this technology. New opportunities have arisen for researchers, unleashing the boundary of human creativity, especially for energy environmental applications such as the production of CH_4 via renewable H_2 and CO_2.

Acknowledgements

The authors would like to thank the Norwegian Ministry of Education and Research and Valide AS through the Plogen Program for financial support.

Conflict of Interest

The authors declare no conflict of interest.

Keywords

CO_2 methanation, hydrotalcite-derived catalysts, Sabatier reaction, structured catalysts, structured reactors

Received: December 20, 2019
Revised: February 27, 2020
Published online: March 25, 2020

[1] B. P. p.l.c, BP Statistical Review of World Energy 2019 (accessed: March 2020).
[2] I. E. Agency, CO_2 Emissions Statistics 2018, www.iea.org/statistics/co2emissions (accessed: March 2020).
[3] A. E. a. Sandbag, The European Power Sector in 2018. Up-to-date analysis on the electricity transition 2019 (accessed: December 2018).
[4] K. Ghaib, F.-Z. Ben-Fares, *Renew. Sustainable Energy Rev.* **2018**, *81*, 433.

[5] S. Rönsch, J. Schneider, S. Matthischke, M. Schlüter, M. Götz, J. Lefebvre, P. Prabhakaran, S. Bajohr, *Fuel* **2016**, *166*, 276.
[6] P. Sabatier, J.-B. Senderens, *Comptes Rendus Des Séances De L'Académie Des Sciences, Section VI Chimie* **1902**, *134*, 514.
[7] A. Muscatello, E. Santiago-Maldonado, in 50th AIAA Aerospace Sciences Meeting including the New Horizons Forum and Aerospace Exposition, American Institute of Aeronautics and Astronautics, Reston, VA **2012**.
[8] T. Schaaf, J. Grünig, M. R. Schuster, T. Rothenfluh, A. Orth, *Energy Sustainability Soc.* **2014**, *4*, 2.
[9] K. Ghaib, K. Nitz, F.-Z. Ben-Fares, *ChemBioEng Rev.* **2016**, *3*, 266.
[10] K. Jalama, *Catal. Rev. Sci. Eng.* **2017**, *59*, 95.
[11] G. A. Mills, F. W. Steffgen, *Catal. Rev. Sci. Eng.* **1974**, *8*, 159.
[12] B. Miao, S. S. K. Ma, X. Wang, H. Su, S. H. Chan, *Catal. Sci. Technol.* **2016**, *6*, 4048.
[13] C. Vogt, M. Monai, G. J. Kramer, B. M. Weckhuysen, *Nat. Catal.* **2019**, *2*, 188.
[14] P. Frontera, A. Macario, M. Ferraro, P. Antonucci, *Catalysts* **2017**, *7*, 59.
[15] M. A. A. Aziz, A. A. Jalil, S. Triwahyono, A. Ahmad, *Green Chem.* **2015**, *17*, 2647.
[16] J. Guo, H. Lou, H. Zhao, D. Chai, X. Zheng, *Appl. Catal. A* **2004**, *273*, 75.
[17] W. Li, H. Wang, X. Jiang, J. Zhu, Z. Liu, X. Guo, C. Song, *RSC Adv.* **2018**, *8*, 7651.
[18] a) M. Younas, L. Loong Kong, M. J. K. Bashir, H. Nadeem, A. Shehzad, S. Sethupathi, *Energy Fuels* **2016**, *30*, 8815; b) J. Gao, Y. Wang, Y. Ping, D. Hu, G. Xu, F. Gu, F. Su, *RSC Adv.* **2012**, *2*, 2358.
[19] E. Baraj, S. Vagaský, T. Hlinčík, K. Ciahotný, V. Tekáč, *Chem. Pap.* **2016**, *70*, 395.
[20] R. Dębek, F. Azzolina-Jury, A. Travert, F. Maugé, *Renew. Sustainable Energy Rev.* **2019**, *116*, 109427.
[21] R. Debek, M. Motak, T. Grzybek, M. Galvez, P. Da Costa, *Catalysts* **2017**, *7*, 32.
[22] a) F. Cavani, F. Trifirò, A. Vaccari, *Catal. Today* **1991**, *11*, 173; b) J. He, M. Wei, B. Li, Y. Kang, D. G. Evans, X. Duan, *Structure and Bonding*, Springer, Berlin, Heidelberg **2006**, pp. 89–119.
[23] G. Fan, F. Li, D. G. Evans, X. Duan, *Chem. Soc. Rev.* **2014**, *43*, 7040.
[24] Z. P. Xu, J. Zhang, M. O. Adebajo, H. Zhang, C. Zhou, *Appl. Clay Sci.* **2011**, *53*, 139.
[25] A. L. Hausberger, C. B. Knight, K. Atwood, *Methanation of Synthesis Gas*, Vol. *146*, American Chemical Society, Washington D.C. **1975**, pp. 47–70.
[26] C. H. Bartholomew, *Appl. Catal. A* **2001**, *212*, 17.
[27] S. Abelló, C. Berrueco, D. Montané, *Fuel* **2013**, *113*, 598.
[28] S. Abate, K. Barbera, E. Giglio, F. Deorsola, S. Bensaid, S. Perathoner, R. Pirone, G. Centi, *Ind. Eng. Chem. Res.* **2016**, *55*, 8299.
[29] L. He, Q. Lin, Y. Liu, Y. Huang, *J. Energy Chem.* **2014**, *23*, 587.
[30] M. Gabrovska, R. Edreva-Kardjieva, D. Crişan, P. Tzvetkov, M. Shopska, I. Shtereva, *React Kinet. Mech. Catal.* **2012**, *105*, 79.
[31] S. Abelló, C. Berrueco, F. Gispert-Guirado, D. Montané, *Catal. Sci. Technol.* **2016**, *6*, 2305.
[32] X. Guo, Z. Peng, M. Hu, C. Zuo, A. Traitangwong, V. Meeyoo, C. Li, S. Zhang, *Ind. Eng. Chem. Res.* **2018**, *57*, 9102.
[33] P. Marocco, E. Alexandru Morosanu, E. Giglio, D. Ferrero, C. Asmelash, A. Lanzini, S. Abate, S. Bensaid, S. Perathoner, M. Santarelli, R. Pirone, G. Centi, *Fuel* **2018**, *225*, 230.
[34] N. Bette, J. Thielemann, M. Schreiner, F. Mertens, *ChemCatChem* **2016**, *8*, 2903.
[35] D. Wierzbicki, R. Baran, R. Dębek, M. Motak, T. Grzybek, M. E. Gálvez, P. Da Costa, *Int. J. Hydrogen Energy* **2017**, *42*, 23548.
[36] J. Liu, W. Bing, X. Xue, F. Wang, B. Wang, S. He, Y. Zhang, M. Wei, *Catal. Sci. Technol.* **2016**, *6*, 3976.
[37] Y. Wang, Y. Xu, Q. Liu, J. Sun, S. Ji, Z.-j. Wang, *J. Chem. Technol. Biotechnol.* **2019**.
[38] X. Wang, T. Zhen, C. Yu, *Appl. Petrochem. Res.* **2016**, *6*, 217.
[39] C. Mebrahtu, S. Perathoner, G. Giorgianni, S. Chen, G. Centi, F. Krebs, R. Palkovits, S. Abate, *Catal. Sci. Technol.* **2019**, *9*, 4023.
[40] T. Burger, F. Koschany, O. Thomys, K. Köhler, O. Hinrichsen, *Appl. Catal. A* **2018**, *558*, 44.
[41] T. Burger, F. Koschany, A. Wenng, O. Thomys, K. Köhler, O. Hinrichsen, *Catal. Sci. Technol.* **2018**, *8*, 5920.
[42] D. Wierzbicki, M. Motak, T. Grzybek, M. E. Gálvez, P. Da Costa, *Catal. Today* **2018**, *307*, 205.
[43] Y. Xu, Y. Chen, J. Li, J. Zhou, M. Song, X. Zhang, Y. Yin, *Int. J. Hydrogen Energy* **2017**, *42*, 13085.
[44] M. Nizio, R. Benrabbah, M. Krzak, R. Debek, M. Motak, S. Cavadias, M. E. Gálvez, P. Da Costa, *Catal. Commun.* **2016**, *83*, 14.
[45] M. K. Titulaer, J. B. H. Jansen, J. W. Geus, *Clays Clay Miner.* **1994**, *42*, 249.
[46] S. Ewald, M. Kolbeck, T. Kratky, M. Wolf, O. Hinrichsen, *Appl. Catal. A* **2019**, *570*, 376.
[47] a) M. Guo, G. Lu, *RSC Adv.* **2014**, *4*, 58171; b) Q. Pan, J. Peng, T. Sun, S. Wang, S. Wang, *Catal. Commun.* **2014**, *45*, 74.
[48] R. Merkache, I. Fechete, M. Maamache, M. Bernard, P. Turek, K. Al-Dalama, F. Garin, *Appl. Catal., A* **2015**, *504*, 672.
[49] a) T. Yoshida, K. Nishizawa, M. Tabata, H. Abe, T. Kodama, M. Tsuji, Y. Tamaura, *J. Mater. Sci.* **1993**, *28*, 1220-; b) M. Tsuji, T. Kodama, T. Yoshida, Y. Kitayama, Y. Tamaura, *J. Catal.* **1996**, *164*, 315.
[50] D. Shi, R. Wojcieszak, S. Paul, E. Marceau, *Catalysts* **2019**, *9*, 451.
[51] C. Mebrahtu, F. Krebs, S. Perathoner, S. Abate, G. Centi, R. Palkovits, *Catal. Sci. Technol.* **2018**, *8*, 1016.
[52] J. Bremer, K. Sundmacher, *React. Chem. Eng.* **2019**, *4*, 1019.
[53] a) A. Cybulski, J. A. Moulijn, *Novel Concepts Catal. Chem. React.* **2010**; b) E. Tronconi, G. Groppi, C. G. Visconti, *Curr. Opin. Chem. Eng.* **2014**, *5*, 55.
[54] T. Boger, A. K. Heibel, *Chem. Eng. Sci.* **2005**, *60*, 1823.
[55] D. Schlereth, P. J. Donaubauer, O. Hinrichsen, *Chem. Eng. Technol.* **2015**, *38*, 1845.
[56] P. H. Ho, M. Ambrosetti, G. Groppi, E. Tronconi, R. Palkovits, G. Fornasari, A. Vaccari, P. Benito, *Studies in Surface Science and Catalysis*, Vol. *178*, Elsevier, Netherlands **2019**, pp. 303–327.
[57] C. J. Navarro, A. M. Centeno, H. O. Laguna, A. J. Odriozola, *Catalysts* **2018**, *8*, 578.
[58] C. Janke, M. S. Duyar, M. Hoskins, R. Farrauto, *Appl. Catal. B.* **2014**, *152–153*, 184.
[59] C. Fukuhara, K. Hayakawa, Y. Suzuki, W. Kawasaki, R. Watanabe, *Appl. Catal. A* **2017**, *532*, 12.
[60] S. Ratchahat, M. Sudoh, Y. Suzuki, W. Kawasaki, R. Watanabe, C. Fukuhara, *J. CO2. Util.* **2018**, *24*, 210.
[61] A. Vita, C. Italiano, L. Pino, P. Frontera, M. Ferraro, V. Antonucci, *Appl. Catal. B.* **2018**, *226*, 384.
[62] P. Biegger, F. Kirchbacher, R. A. Medved, M. Miltner, M. Lehner, M. Harasek, *Energies* **2018**, *11*, 1679.
[63] D. Schollenberger, S. Bajohr, M. Gruber, R. Reimert, T. Kolb, *Chem. Ing. Tech.* **2018**, *90*, 696.
[64] J. Y. Ahn, S. W. Chang, S. M. Lee, S. S. Kim, W. J. Chung, J. C. Lee, Y. J. Cho, K. S. Shin, D. H. Moon, D. D. Nguyen, *Fuel* **2019**, *250*, 277.
[65] M. Shima, Y. Sakurai, M. Sone, A. Ohnishi, T. Yoneda, T. Abe, *Int. J. Microgravity Sci. Appl.* **2013**, *30*, 86.
[66] Y. Li, Q. Zhang, R. Chai, G. Zhao, Y. Liu, Y. Lu, F. Cao, *AlChE J.* **2015**, *61*, 4323.
[67] S. Tada, S. Ikeda, N. Shimoda, T. Honma, M. Takahashi, A. Nariyuki, S. Satokawa, *Int. J. Hydrogen Energy* **2017**, *42*, 30126.
[68] M. Frey, D. Édouard, A.-C. Roger, *C. R. Chim.* **2015**, *18*, 283.
[69] M. Frey, T. Romero, A.-C. Roger, D. Edouard, *Chem. Eng. Sci.* **2019**, *195*, 271.
[70] M. Frey, T. Romero, A.-C. Roger, D. Edouard, *Catal. Today* **2016**, *273*, 83.

[71] M. Frey, A. Bengaouer, G. Geffraye, D. Edouard, A.-C. Roger, *Energy Technol.* **2017**, *5*, 2078.
[72] A. Bengaouer, J. Ducamp, I. Champon, R. Try, *Can. J. Chem. Eng.* **2018**, *96*, 1937.
[73] A. Ricca, L. Truda, V. Palma, *Chem. Eng. J.* **2019**, *377*, 120461.
[74] C. Fukuhara, S. Ratchahat, A. Kamiyama, M. Sudoh, R. Watanabe, *Chem. Lett.* **2019**, *48*, 441.
[75] J. A. H. Lalinde, J. Jiang, G. Jai, J. Kopyscinski, *Chem. Eng. J.* **2019**, *357*, 435.
[76] J. A. H. Lalinde, K. Kofler, X. Huang, J. Kopyscinski, *Catalysts* **2018**, *8*, 86.
[77] G. A. Jarvi, K. B. Mayo, C. H. Bartholomew, *Chem. Eng. Commun.* **1980**, *4*, 325.
[78] J. G. Khinast, A. Bauer, D. Bolz, A. Panarello, *Chem. Eng. Sci.* **2003**, *58*, 1063.
[79] S. Specchia, C. Galletti, V. Specchia, *Studies in Surface Science and Catalysis*, Vol. *175*, Elsevier, Netherlands **2010**, pp. 59–67.
[80] J. Ducamp, A. Bengaouer, P. Baurens, *Can. J. Chem. Eng.* **2017**, *95*, 241.
[81] S. Danaci, L. Protasova, J. Lefevere, L. Bedel, R. Guilet, P. Marty, *Catal. Today* **2016**, *273*, 234.
[82] S. Danaci, L. Protasova, F. Snijkers, W. Bouwen, A. Bengaouer, P. Marty, *Chem. Eng. Process* **2018**, *127*, 168.
[83] S. Danaci, L. Protasova, V. Middelkoop, N. Ray, M. Jouve, A. Bengaouer, P. Marty, *React. Chem. Eng.* **2019**, *4*, 1318.
[84] V. Middelkoop, A. Vamvakeros, D. de Wit, S. D. M. Jacques, S. Danaci, C. Jacquot, Y. de Vos, D. Matras, S. W. T. Price, A. M. Beale, *J. CO2. Util.* **2019**, *33*, 478.
[85] V. Middelkoop, K. Coenen, J. Schalck, M. Van Sint Annaland, F. Gallucci, *Chem. Eng. J.* **2019**, *357*, 309.
[86] V. Gokhale Sagar, K. Tayal Rajiv, K. Jayaraman Valadi, D. Kulkarni Bhaskar, *Int. J. Chem. React. Eng.* **2005**, *3*.
[87] O. Görke, P. Pfeifer, K. Schubert, *Catal. Today* **2005**, *110*, 132.
[88] J. Hu, K. P. Brooks, J. D. Holladay, D. T. Howe, T. M. Simon, *Catal. Today* **2007**, *125*, 103.
[89] K. P. Brooks, J. Hu, H. Zhu, R. J. Kee, *Chem. Eng. Sci.* **2007**, *62*, 1161.
[90] Y. Men, G. Kolb, R. Zapf, V. Hessel, H. Löwe, *Catal. Today* **2007**, *125*, 81.
[91] Z. Liu, B. Chu, X. Zhai, Y. Jin, Y. Cheng, *Fuel* **2012**, *95*, 599.
[92] N. Engelbrecht, S. Chiuta, R. C. Everson, H. W. J. P. Neomagus, D. G. Bessarabov, *Chem. Eng. J.* **2017**, *313*, 847.
[93] S. Chiuta, R. C. Everson, H. W. J. P. Neomagus, D. G. Bessarabov, *Int. J. Hydrogen Energy* **2015**, *40*, 2921.